Fall 2021

Building Intuition for Quantum Information using 3D-Printing

Louis R Nemzer

Building Intuition for Quantum Information using 3D-Printing

"I thought of calling it 'information,' but the word was overly used, so I decided to call it 'uncertainty'. When I discussed it with John von Neumann, he had a better idea. Von Neumann told me, 'You should call it entropy… nobody knows what entropy really is, so in a debate you will always have the advantage." – Claude Shannon

"Quantum mechanics, at its core, is a change to the rules of probability - and this is also where the power of quantum computing comes from - these different rules of probability than the ones that we are used to." — Scott Aaronson[1]

Abstract

Quantum computing is poised to revolutionize the fields of cryptography, optimization, and rational drug design. However, forming the proper intuition for quantum phenomena, even by experienced practitioners, is often difficult. This is due in large part to the impossibility of simple visualizations of even basic elements, such as two-qubit entangled states or complex time-varying spatial wavefunctions. This problem can be compounded by a lack of clarity of fundamental quantum and information theoretic principles, especially Bell's Theorem and the definition of entropy. Here, examples of 3D-Printed visualizations – including of the von Neumann entropy of two-qubit states and the time-evolution of the probability density in an anisotropic harmonic oscillator – are used to help elucidate the underlying foundations of quantum information theory, and the distinction between quantum and classical correlations. With an emphasis on physical visualizations, this approach may lead to progress in both pedagogy and the design of quantum computers.

Motivation

Quantum computing[2] holds the promise of making use of the deeply counterintuitive rules of quantum mechanics (QM) to perform certain computational tasks much more quickly than current hardware. Many quantum computing methods, such as Shor's algorithm, rely on the ability for interference effects to cancel all but the correct answer.[3] The members of the workforce of the future who are in line to design, build, program, and operate these quantum computers are being trained now. They will need a foundation in Quantum Information Science and Technology (QIST), which builds on concepts from information theory, computer science, and quantum mechanics.[4] Cultivating an intuitive understanding of practical QIST principles may be more critical for these aspiring students compared with abstract quantum theory.[5,6] However, existing educational resources often require a considerable time investment before they can even approach problems related with QIST.[7] Recently, government funding in this area has increased dramatically, as with the National Q-12 Education Partnership, with the goal of increasing the technical ability of students.[8] Similarly, Europe's Quantum Flagship initiative[9] released a Competence Framework for Quantum Technologies, which lists foundational concepts of quantum physics that may be unfamiliar to first-time students, including superposition, time evolution, entanglement, and Bell inequalities.[10] Much of the effort by educators to date has been focused on helping students intuitively picture the quantum wavefunction.[11] Some existing computer-generated visualizations use color to show the complex phase, and use brightness for the amplitude.[12] Other simulations are interactive, and allow students to see the time evolution of the wavefunction in a system with a chosen Hamiltonian, as with Quantum Composer.[13] These are very useful classroom tools, but remain limited to two dimensions. Having physical models to hold and manipulate can help make quantum concepts more intuitive for students.

Introduction

Quantum mechanics is our best theory for the laws of physics at small scales, and has - with an incredible degree of precision - successfully passed every experimental test to date. Without it, we would not have laptops, smartphones, MRI machines, microprocessors, or lasers. Most properties of materials, like electrical conductivity or magnetism, are direct results of QM, and some experimental values have been determined to a precision of a few parts per trillion. At the same time, somewhat disconcertingly, QM fundamentally challenges our native conceptions of causality,[14] and in particular, it scrambles intuitive understandings of what is deterministic and what is probabilistic. For example, the Heisenberg Uncertainty principle famously states that knowledge of one observable, like the position of a particle, precludes prefect knowledge of a corresponding quantity, in this case, its momentum. However, in between measurements, the wavefunction describing that particle evolves perfectly deterministically according to the Schrödinger wave equation. Similarly, the Stern-Gerlach experiment, first performed almost a century ago, showed that measurement of an electron's spin along a chosen axis will always be one of two possibilities: up or down. Furthermore, the value will not change if measured repeatedly in the same direction, but once measured in a perpendicular direction, all information of the original axis will be destroyed. Subsequently, measurements will yield up or down randomly with equal probability. In other words, there is an inherent paradox in our understanding of the laws that govern our Universe. Even if we know everything about the wavefunction - which is everything *there is* to know according to most interpretations of quantum mechanics - and its evolution in time is completely deterministic, the outcomes are still inherently probabilistic, and only give the chances to find a particle in every particular location if we would choose to look. That is, once we make a measurement, we cannot be sure of the outcome, only the *a priori* probabilities for each. Building an intuition about what is probabilistic and what is deterministic in this brave new world of QM is crucial for the success of quantum computing.

Moreover, particles can be described as existing in a superposition of states simultaneously, but these representations are not unique. In general, a wavefunction can be in a single deterministic state when measured in one direction, but will be in a probabilistic superposition when measured in others. This leads to strange outcomes, even for those well versed in probability theory. In a classical system, uncertainty about a part - as measured by the information entropy associated with that subset - will inevitably lead to an uncertain whole. However, quantum entropy obeys subadditivity[15] in which non-classical correlations due to entanglement can remove all doubt when the total wavefunction is considered. It has been proven that any advantage a quantum computer has over its classical counterpart can only come from entanglement between quantum bits (qubits). Entanglement is another inescapable part of QM with no classical analogue. According to Bell's Theorem,[16] quantum entanglement gives rise to correlations[17] between measurements on different particles, even after being separated by great distances, and cannot be explained with classical hidden variables[18] adhering to local realism. Entanglement[19] is now seen as a resource[20] within quantum computing, to be protected from processes that would cause decoherence of the wavefunction and a return to classical behavior.

What follows are examples of basic ideas from quantum mechanics that resist conventional representation due to fundamental limitations imposed by the rules of physics. For each example, a new method of 3D visualization is presented to help provide a more intuitive understanding compared with previous pedagogical approaches. First, an intuitive explanation of Bell's theorem, which rules out the possibility of local realism with hidden variables, is provided using a 3D-printed model of the experimental apparatus. Then, a 3D-printed "map" is shown of entangled two-qubit states obtainable using a CNOT gate,[21] a basic process in quantum computing. While a single qubit can be described in three dimensions with a Bloch sphere, the complexity and correlations of even just two entangled qubits cannot be simply visualized.[22] This is a fundamental limitation even for quantum computer visualizations, like Quirk,[23] that track of the wavefunction throughout the circuit. To represent entangled bipartite states, a 3D-printed density matrix is also presented. Finally, the deterministic time-evolution of the probability density of a particle in a two-dimensional anisotropic harmonic potential is represented with a 3D visualization. An emphasis is placed on explicitly distinguishing between classical and quantum correlations. 3D-printable .stl files and associated movie animations are provided in the Supplementary Material, along with an appendix showing the output from a test of entanglement run on a real quantum computer hosted by IBM Quantum Lab.[24]

Background

Density Matrix

In quantum mechanics, the Bloch Sphere representation of a single qubit maps any pure state $|\psi\rangle$ onto a point on the surface of a unit sphere:

$$|\psi\rangle \;=\; \cos\frac{\theta}{2}|0\rangle + e^{i\varphi}\sin\frac{\theta}{2}|1\rangle \qquad (1)$$

The probabilities of measuring 0 or 1 are $|\langle 0|\psi\rangle|^2 = \left(\cos\frac{\theta}{2}\right)^2$ and $|\langle 1|\psi\rangle|^2 = \left(\sin\frac{\theta}{2}\right)^2$, respectively. Mixed single-particle states, which consist of classical mixtures of pure states, can still be represented this way, but as points on the interior of the unit ball. The density matrix ρ for a pure state $|\psi\rangle$ can be calculated using:

$$\rho_\psi = \sum_i |\psi_i\rangle\langle\psi_i| \qquad (2)$$

The density matrix contains all observable information by giving the probability of each outcome when measured in any direction. The density matrix is not unique, and can be obtained from various combinations of mixed states. The amplitude of the projection of state $|\psi\rangle$ along the direction of the basis vector $|v\rangle$ is the inner product between them, $\langle v|\psi\rangle$. The Born rule says that the probability of measuring "up" when making this measurement is amplitude squared:

$$P(v_\psi) = \langle v|\psi\rangle\langle\psi|v\rangle = |\langle v|\psi\rangle|^2 \qquad (3)$$

From the definition of the density matrix (eq. 2) this can be obtained with:

$$P(v_\psi) = \langle v|\rho_\psi|v\rangle \qquad (4)$$

And, for any observable represented by the Hermitian matrix A, the expectation value can be calculated by:

$$\langle A\rangle = tr(A\rho_\psi) \qquad (5)$$

where tr is the trace operator. In this way, the density matrix contains all accessible information regarding measuring along any desired axis.[25] However, this is not a complete description of the state, since there is an upper bound[26] on how much information can be extracted from a quantum system. Essentially, each qubit can convey, at most, one bit information. Also, the "no-cloning" theorem enforces that only one of these measurements can be done before the state is irreparably changed. The density matrices of classical mixtures contain only diagonal entries, and can be thought of classical probability distributions. Off-diagonal entries show quantum interference effects between states. Correlations in a classical mixture are constrained by Bell inequalities (local realism) that can fit within a Venn diagram, as shown below.

A qubit in a superposition of pure states differs from a classical probability mixture in that there will be an axis for which the outcome will be certain. For example, the superposition $|+\rangle = \frac{1}{\sqrt{2}}(|0\rangle + |1\rangle)$ has the density matrix:

$$\rho_+ = \frac{1}{2}\begin{pmatrix} 1 & 1 \\ 1 & 1 \end{pmatrix} \qquad (6)$$

As opposed to the classical mixture of equal probability of 0 and 1, which is the maximally mixed state:

$$\rho_{mix} = \frac{1}{2}\begin{pmatrix} 1 & 0 \\ 0 & 1 \end{pmatrix} \qquad (7)$$

Notice only diagonal entries are nonzero for the classical mixture. When measured in the standard $\{|0\rangle, |1\rangle\}$ basis, both ρ_+ and ρ_{mix} give up and down with equal probability. In fact, if only observed along the standard basis, it is not possible to distinguish between them. However, measured in its own basis, the pure superposition $|+\rangle$ state always gives the same answer, while the maximally mixed state always gives equal chance for up and down in every possible basis.

Information Entropy

Entanglement is a nonclassical correlation between particles that occurs when the joint wavefunction cannon be written as the product of single-particle wavefunctions. The degree of entanglement between qubits can be quantified using information theory, which focuses on how the amount of uncertainty changes in a system. Classical information theory due to Claude Shannon recognizes the deep connections between thermodynamic entropy – which is conventionally described as a measure of disorder in a system or energy unavailable to do work – and the information content of a message. In fact, the formula is the same:[27]

$$S = -\sum_i p_i \log_2 p_i \qquad (8)$$

where p_i is the probability of finding the system in state *i*. Fundamentally, entropy is the "missing information"[28,29] that is needed to specify the exact state of a system given a partial description.[30] As surprising as it may sound, entropy is not an intrinsic property of systems, although it is an extremely useful one. Entropy only enters the picture because of our insistence on grouping together similar microstates, according to some average value, in collections called macrostates. For thermodynamics, this is not as much a choice as it is a necessity, since keeping track of the positions and momenta of even a handful of particles quickly becomes impossible, let alone the unimaginably large computing resources required to completely monitor the state of all the air molecules bouncing around a normal sized room. The best we can do, practically, is monitor macroscopic variables like the temperature, pressure, and volume, *et cetera*. Entropy tells us how much information is lost by referring to an averaged macrostate instead of identifying the exact microstate. More specifically, the entropy is equal to the average number of binary questions required determine the exact state if given the ensemble it belong to.[31] Because of this, Jaynes showed that entropy is in the "eye of the beholder,"[32] and that having more complete information can be converted into energy.[33] In particular, Maxwell's Demon[34] has the ability to turn information into useful work via a Szilárd Engine.[35] On the other hand, Laplace's Demon,[36] who by definition knows everything, doesn't care about entropy at all.

The quantum analogue of Shannon's formula is the van Neumann entropy:

$$S = -tr(\rho \ln \rho) = -\sum_i \lambda_i \ln \lambda_i \qquad (9)$$

where λ_i are the eigenvalues of ρ. Since the wavefunction is all there is to know about state, pure states have zero entropy. This leads to the *subadditivity* of quantum information, since the van Neumann entropy measures the loss of information by knowing only the individual wavefunctions and not the "wavefunction of the Universe."[37] While classical uncertainty, as quantified by the Shannon entropy, can never be less than sum of its constituent parts, there can be entangled quantum states - with zero van Neumann entropy as a whole - that each have nonzero entropy individually. For example, it has been shown that you can be completely

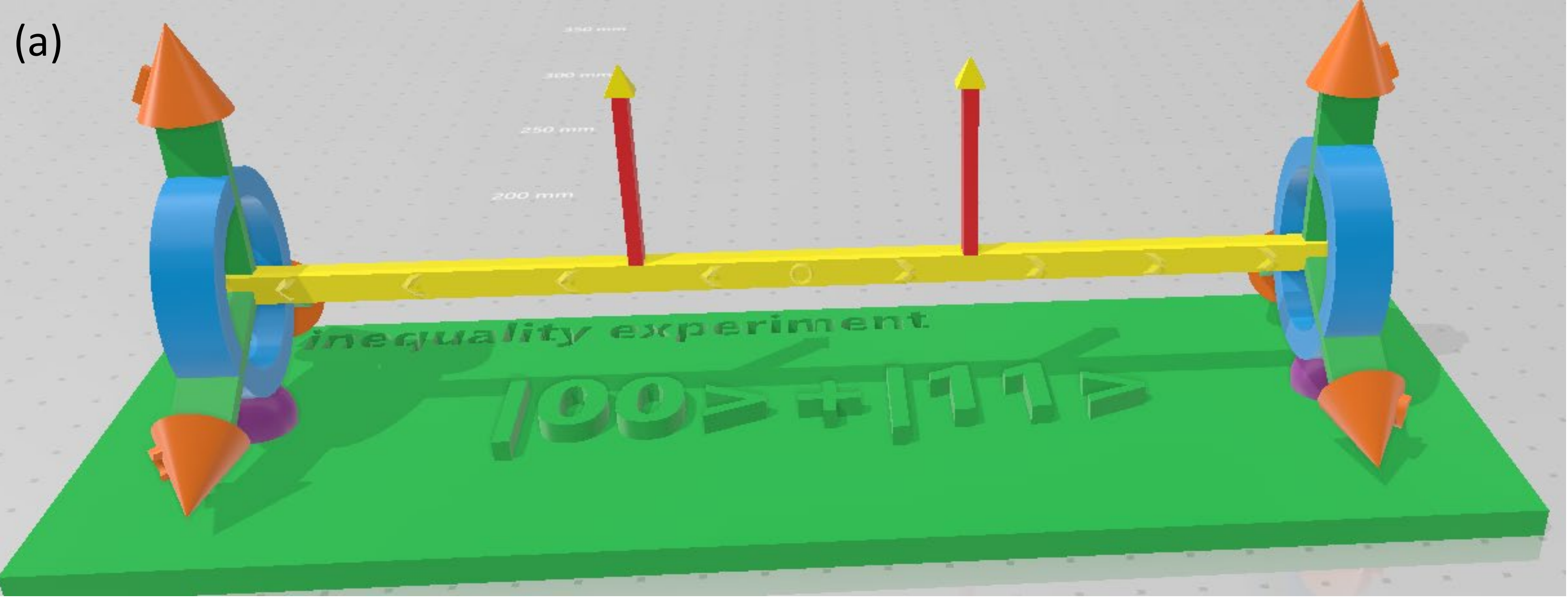

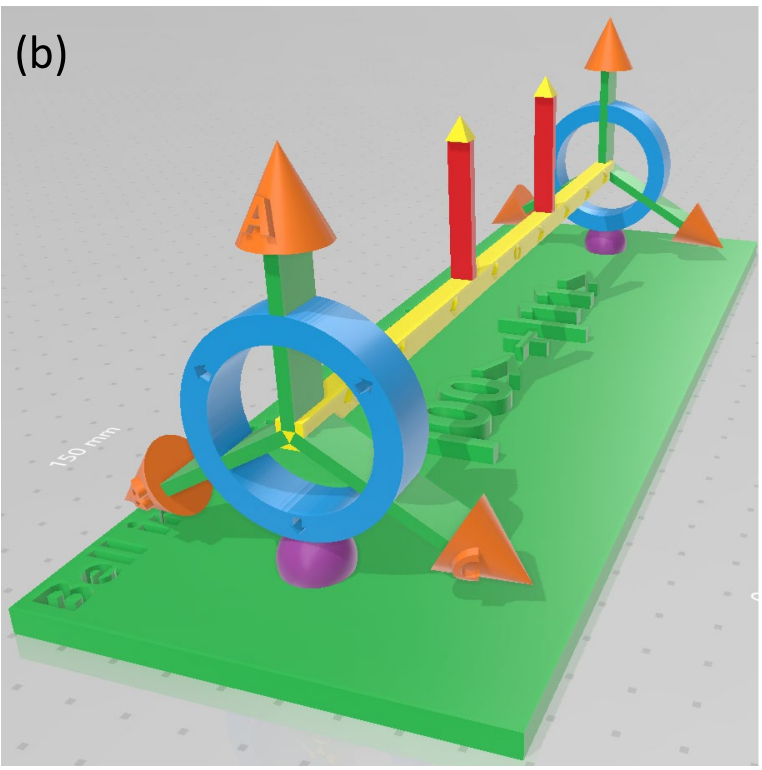

Figure 1: *Bell test apparatus visualization and 3D-Printed model. During such an experiment, an entangled pair of spin-1/2 particles, represented by the arrows, are created at the center. One particle travels to each detector. Each detector can be set to measure along axis A. B, or C.*

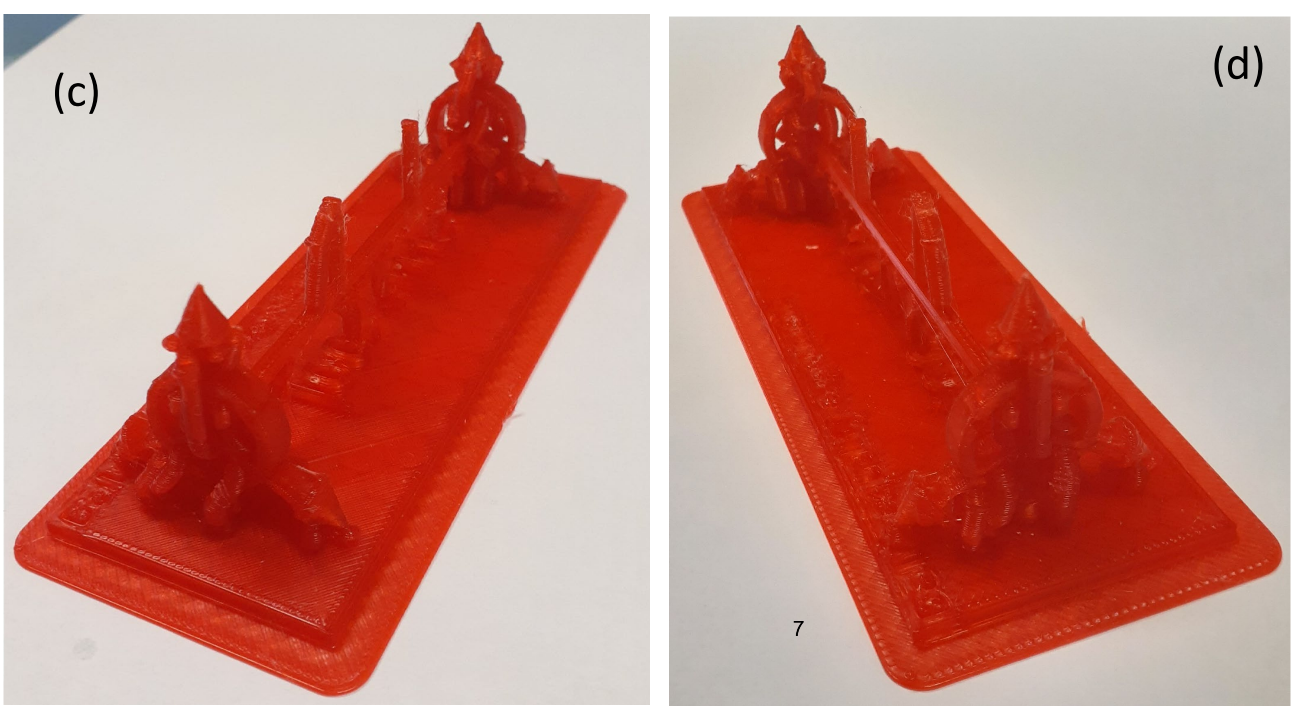

ignorant of the joint wavefunction, yet no one can point to a single part you are unsure about.[38] Overall, the value of S gives the minimum Shannon entropy among all possible probability distributions from all possible measurement bases.[39] In short, classical entropy is the cost of thinking in terms of the "big picture" instead of individual particles. Quantum mechanics inverts this view, in the sense that the joint wavefunction can contain information about correlations between particles that is absent from the "atomized" single-particle wavefunctions.

Bell Test Apparatus

Given its centrality in quantum theory, a strong understanding Bell's Inequality, which sets a limit on hidden variable theories - and how it is violated by entangled particles - is crucial. Bell's theorem shows that any explanation of the Universe that adheres to local realism has unavoidable constraints on the correlations between measurements. A 3D-printed model of a Bell Test apparatus is shown in figure 1. Pairs of particles are created at the center, and each one is sent to a separate detector. In this version of the experiment, each detector can be set independently in one of three evenly-spaced settings, denoted A, B, and C (Figure 2). The direction of "up" or $|0\rangle$ for each detector setting is represented by the corresponding letter, while the "down" or $|1\rangle$ state has an overbar. When a pair of entangled particles prepared in the entangled $|\Phi^{+}\rangle = \frac{1}{\sqrt{2}}[|00\rangle + |11\rangle]$ state are both measured in the same direction, experiments have shown that the detectors always give the same result, either both up or both down:

$$SAME_{AA} = SAME_{BB} = SAME_{CC} = 1 \tag{10}$$

When measured repeatedly along different axes, any hidden variables theory in which the particles have well-defined properties at all times will be limited by Bell's inequality. This can be stated as:

$$SAME_{AB} + SAME_{AC} + SAME_{BC} \geq 1 \tag{11}$$

There are several ways of understanding this result. By logical consistency, the number of matches is restricted to be an odd number, either 1 or three. Exactly two is impossible, for example, if A=B and B=C, then A=C by the transitive property. Similarly, there cannot be zero matches, by geometrical frustration[40] (fig 3). That is, if A ≠ B and B ≠ C, then A = C is inevitable. Even more intuitively, figure 4 shows how a hidden variables theory, which must generate logically consistent Venn diagrams, leads unavoidably to Bell's Theorem.[41] Adding the probabilities of the three circles encompasses all possible outcomes at least once. By the axioms of probability, this must sum to at least 1. Alternatively, this can be seen by enumerating all possible hidden variable values (Table 1).

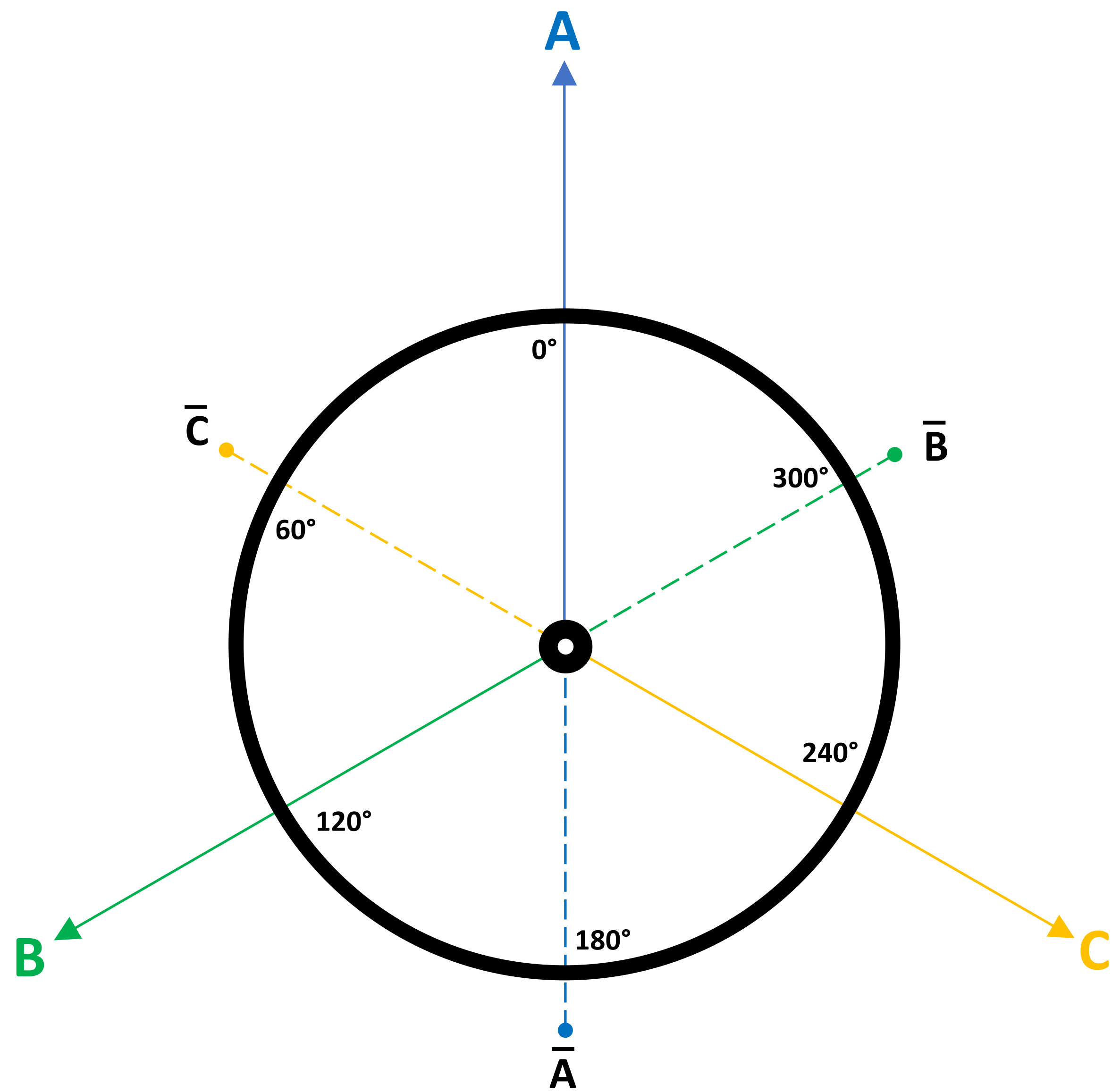

FIGURE 2: *Settings for each detector in the Bell test apparatus. The letter shows the detector setting representing "up", while the letter with an overbar shows "down" for that axis.*

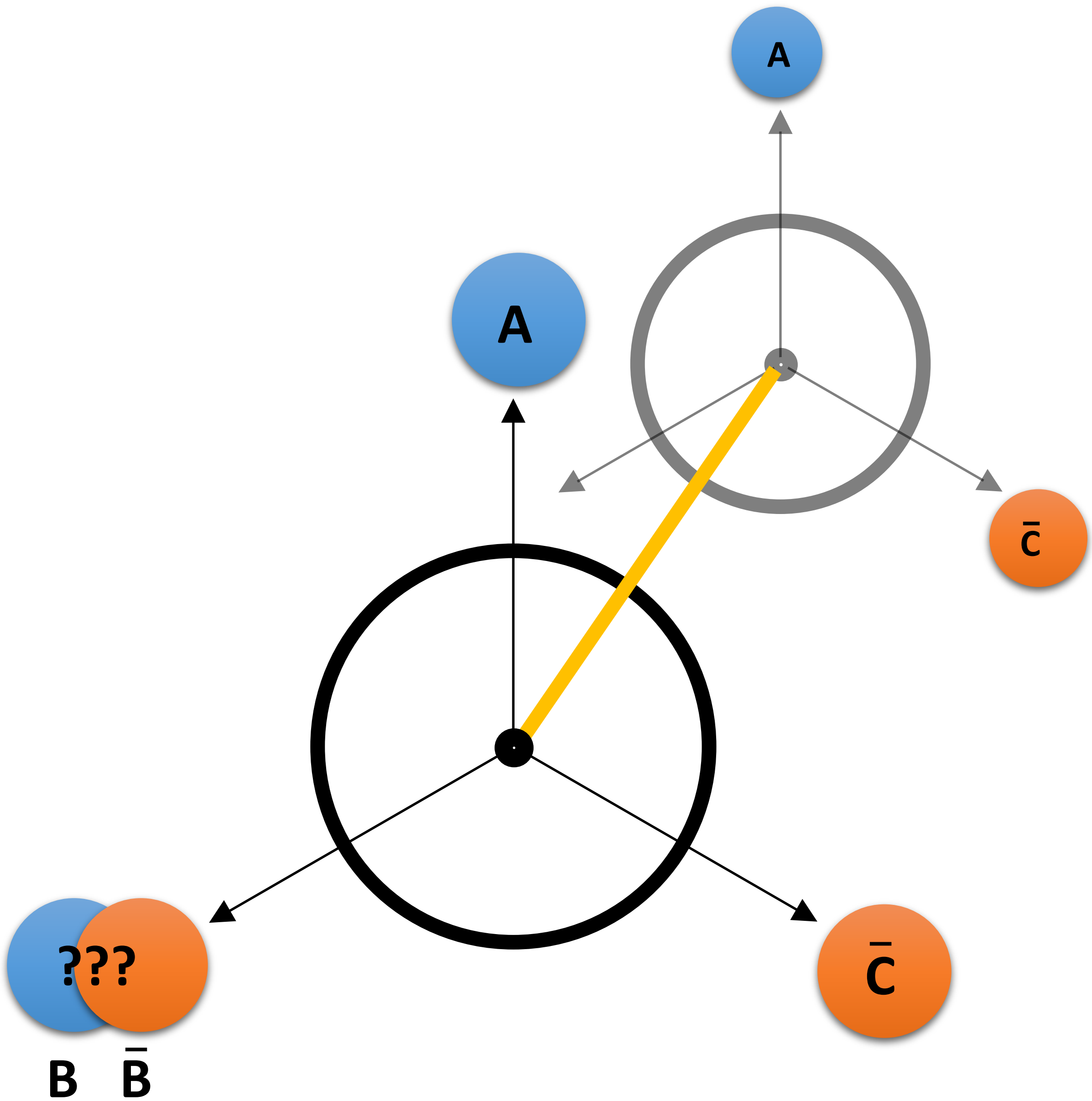

FIGURE 3: *Illustration of the geometric frustration that prevents AB, BC, and AC from all being different simultaneously.*

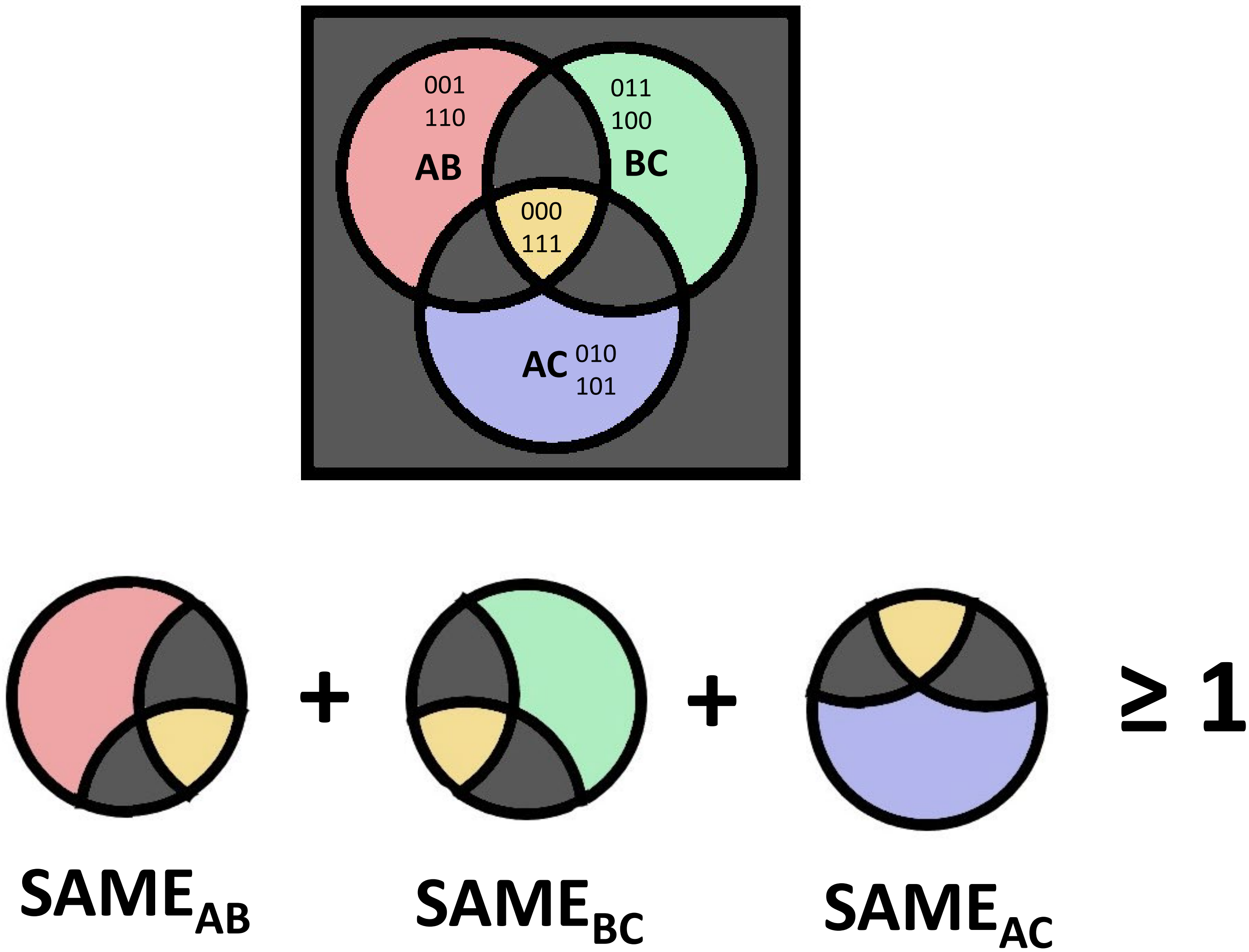

FIGURE 4: *Graphical proof of Bell's Theorem using a Venn diagram. Any hidden variables theory that assigns definite values to each outcome will include every possibility at least once.*

Hidden Variables				SAME?			
A	**B**	**C**		**AB**	**BC**	**AC**	**# Same**
0	0	0		✓	✓	✓	3
0	0	1		✓			1
0	1	0				✓	1
0	1	1			✓		1
1	0	0			✓		1
1	0	1				✓	1
1	1	0		✓			1
1	1	1		✓	✓	✓	3

TABLE 1: All possible hidden variables enumerated, subject to the constraint that both particles give the same value when measured along the same direction. The total number of matches when measured in the AB, BC, and AC directions is always one or greater.

Many empirical tests have confirmed that these limits can be violated by entangled particles, performed with increasing stringency to close any conceivable loophole[42,43,44]. However, it is important to understand why the entangled state $\frac{1}{\sqrt{2}}(|00\rangle + |11\rangle)$ violates Bell's theorem, while a classical mixture of a 50% chance of $|00\rangle$ and 50% chance of $|11\rangle$ does not. Figure 5 illustrates the probabilities that the detectors give the same result, either (a) up or (b) down. In these diagrams, the near detector is set along the A axis, and the far detector is set to B. If the near detector measures $|0\rangle$, which is up in the A direction, the wavefunction at the far detector collapses to $|0\rangle$ as well. Or, as explained by interpretations of quantum mechanics that do not involve wavefunction collapse, such as "consistent histories"[45] or Everett's Many Worlds,[46] only results that accord with the original entangled wavefunction are ever observed. This happens half of the time, and when it does the far detector offset by 120° at B will measure up with probabilty

$$P(\psi, v) = \cos^2\left(\frac{\Delta\theta}{2}\right) = \cos^2\left(\frac{120}{2}\right) = \frac{1}{4} \qquad (12)$$

of the time. As a result, both up (figure 5a) will occur $\frac{1}{2}\left(\frac{1}{4}\right) = \frac{1}{8}$ of the time. The same will be true for both down (figure 5b), and the total value of $SAME_{AB}$ will be P(Both Up) + P(Both Down) $=2\left(\frac{1}{8}\right) = \frac{1}{4}$. The total is then $SAME_{AB} + SAME_{AC} + SAME_{BC} = \frac{3}{4}$, which is less than the Bell Limit

(a)

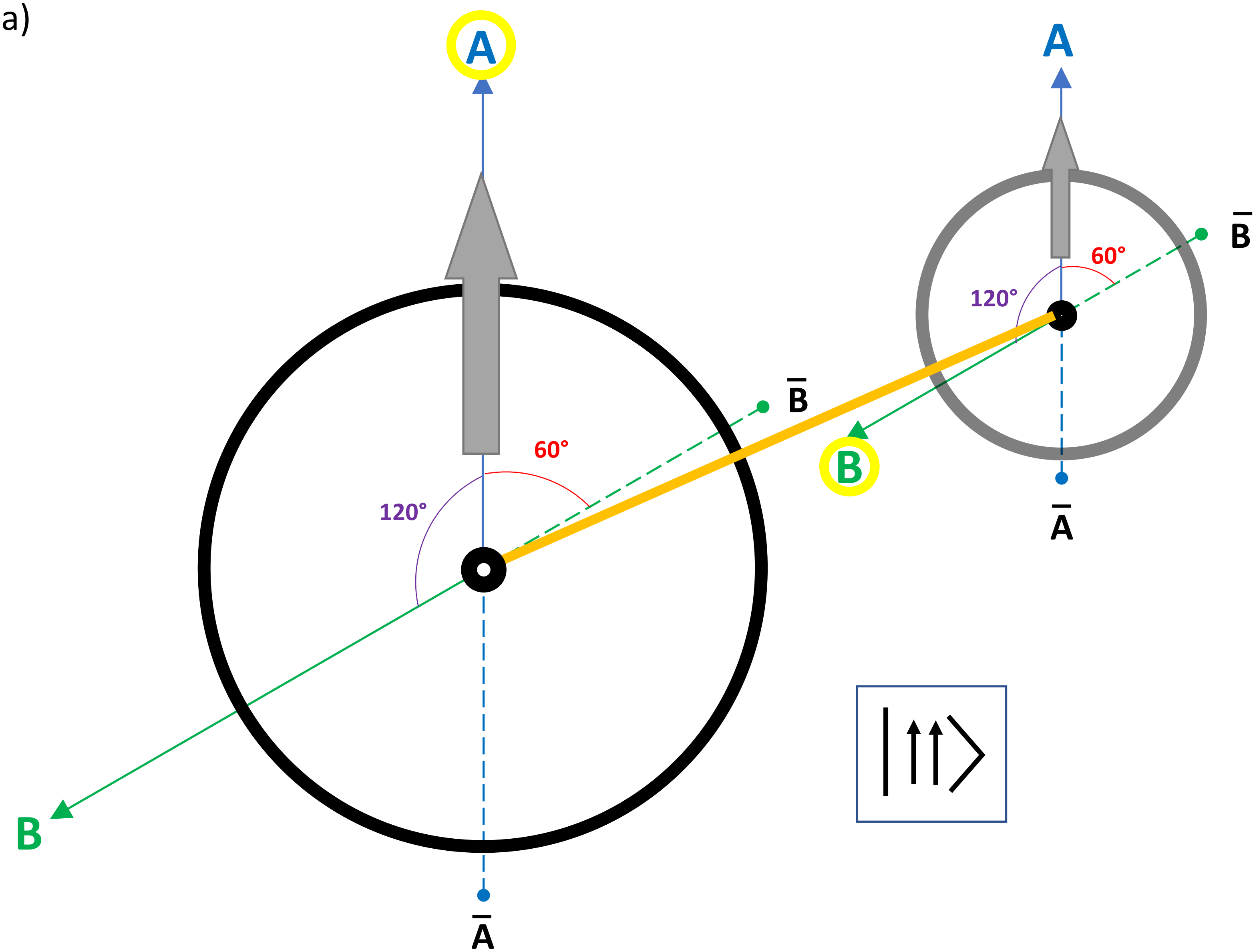

(b)

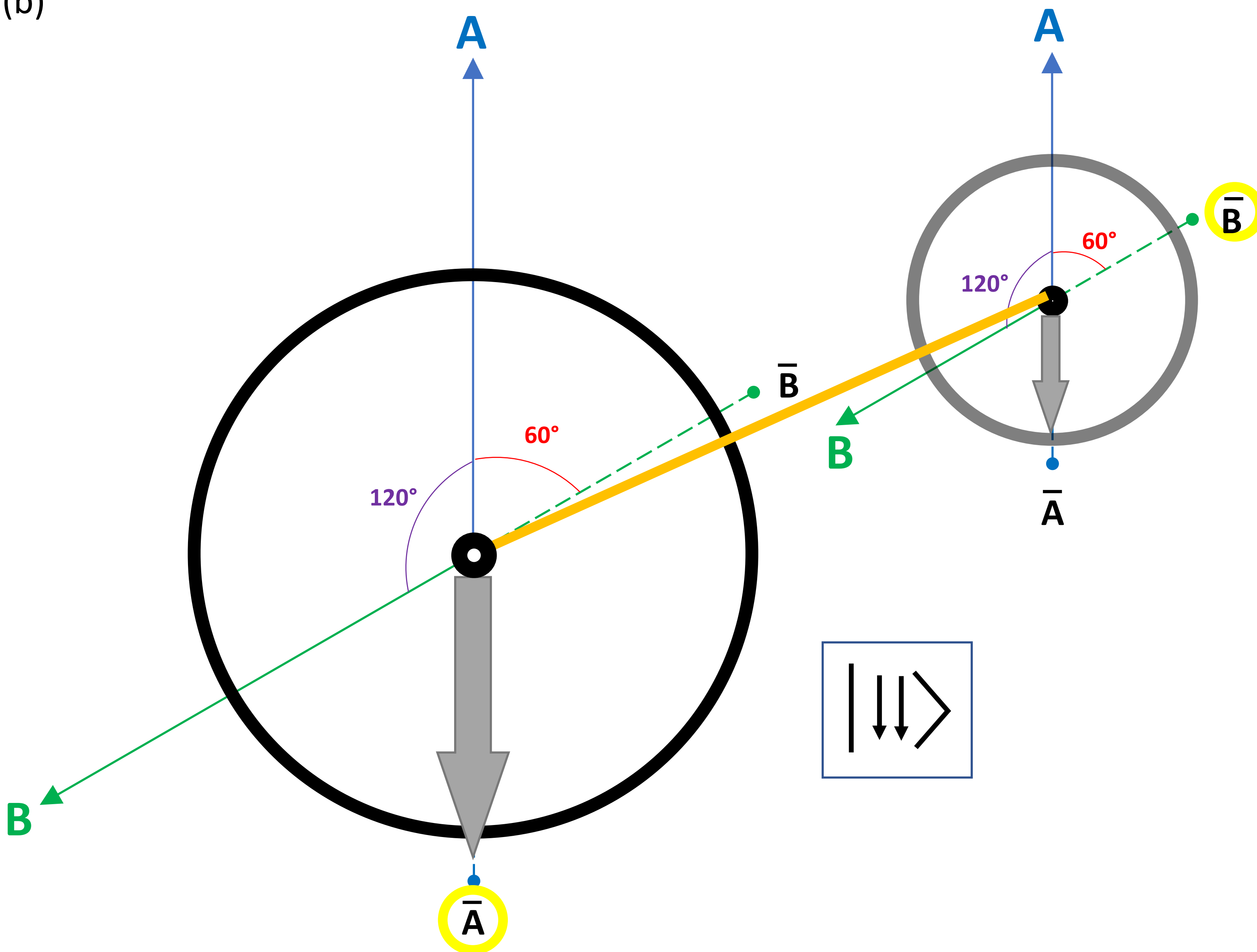

FIGURE 5: *Calculating the probability of $SAME_{AB}$ when both are measured to be (a) up or (b) down.*

of 1. In contrast, a classical mixture in which a pair of unentangled particles is generated with an equal probability of both being up or both being down will not violate Bell's inequality (Table 2).[47]

Value	Detector 1	Detector 2	Result	Entangled (|00>+|11>)/√2		Classical Mixture ½|00> and ½|11>	
				|00>	|11>	|00>	|11>
$SAME_{AB}$	A	B	↑↑	1/8	0	1/8	0
	A	B	↓↓	0	1/8	0	1/8
$SAME_{AC}$	A	C	↑↑	1/8	0	1/8	0
	A	C	↓↓	0	1/8	0	1/8
$SAME_{BC}$	B	C	↑↑	1/32	3/32	1/32	9/32
	B	C	↓↓	3/32	1/32	9/32	1/32
			TOTAL	3/4 = 0.75		9/8 = 1.125	

TABLE 2: Comparing the results of a Bell test using entangled particles or a classical mixture. The probability that the detects give the same result, either both "up" or both "down," are computed. Only entangled states can violate the Bell inequality to be less than 1.

Two-Qubit Entanglement Entropy

To generate the entangled qubits in a quantum computer, both are initialized in the $|0\rangle$ state. A Hadamard Gate is applied to the top qubit, which converts it into $|+\rangle = \frac{1}{\sqrt{2}}(|0\rangle + |1\rangle)$. Then, a CNOT gate is applied between the qubits, with the top qubit as the control and the bottom qubit as the target (figure 6a). The action of the CNOT gate flips the target qubit if the control is in the $|1\rangle$ state, and otherwise does nothing. This yields the desired bell state $|\Phi^+\rangle = \frac{1}{\sqrt{2}}[|00\rangle + |11\rangle]$.

In the two-qubit basis $\begin{bmatrix} |00\rangle \\ |01\rangle \\ |10\rangle \\ |11\rangle \end{bmatrix}$, the bell state can be expressed as:

$$|\Phi^+\rangle = \frac{1}{\sqrt{2}}\begin{bmatrix} 1 \\ 0 \\ 0 \\ 1 \end{bmatrix} \qquad (13)$$

The appendix shows the results creating and measuring an entangled bell state on real quantum computer. As a generalization of the Bell test, instead of applying a Hadamard Gate, we allow the

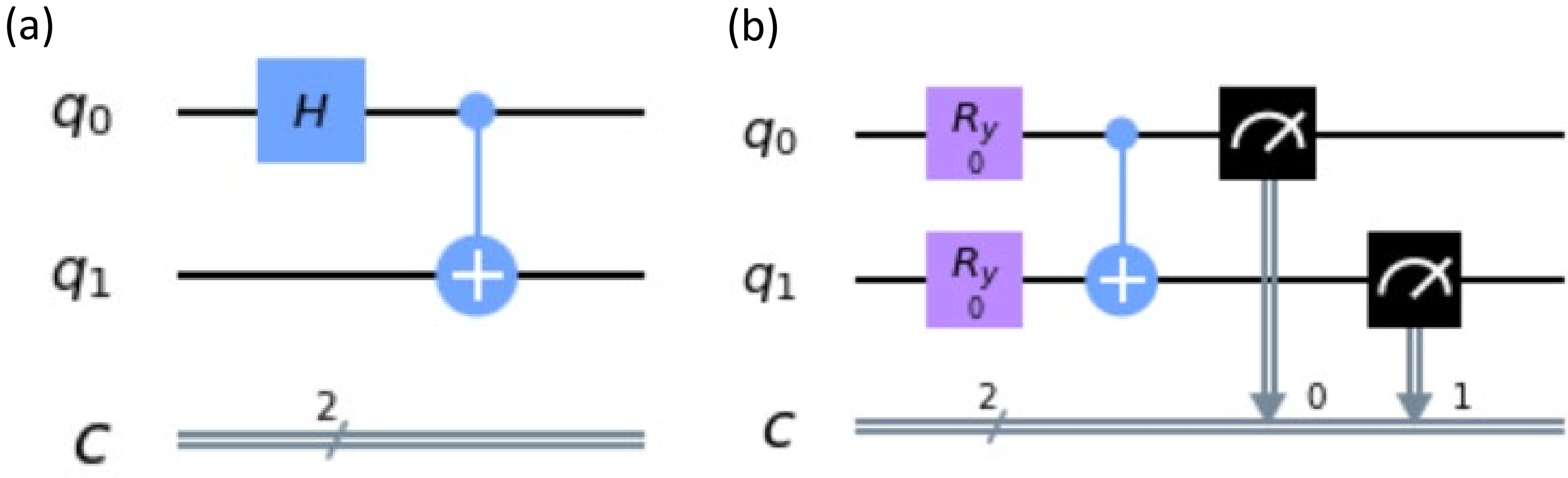

FIGURE 6: *Quantum Circuit in Qiskit. (a) Simple circuit for generating a Bell State (b) Generalized circuit for producing partially entangled states.*

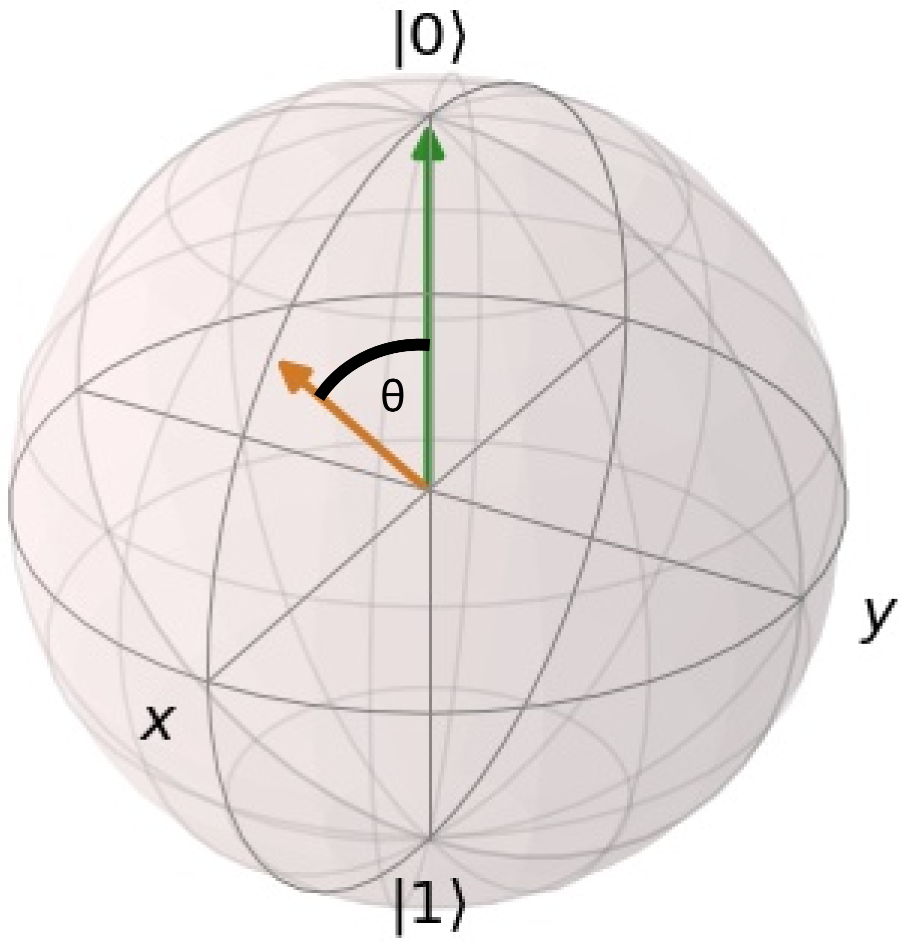

FIGURE 7: *Bloch sphere representation of a single qubit.*

input states to vary prior to applying the CNOT gate. This is accomplished using independently set R_y gates for each qubit, as shown in figure 6b. The Ry gates rotate each qubit by θ (figure 7). Setting ϕ=0 for both qubits, we get the input product state

$$|\psi_A\rangle\otimes|\psi_B\rangle = \cos\frac{\theta_A}{2}\cos\frac{\theta_B}{2}|00\rangle + \cos\frac{\theta_A}{2}\sin\frac{\theta_B}{2}|01\rangle + \sin\frac{\theta_A}{2}\cos\frac{\theta_B}{2}|10\rangle + \sin\frac{\theta_A}{2}\sin\frac{\theta_B}{2}|11\rangle \tag{14}$$

The input state can be expressed as:

$$|\psi_A\rangle\otimes|\psi_B\rangle = \begin{bmatrix} \cos\frac{\theta_A}{2}\cos\frac{\theta_B}{2} \\ \cos\frac{\theta_A}{2}\sin\frac{\theta_B}{2} \\ \sin\frac{\theta_A}{2}\cos\frac{\theta_B}{2} \\ \sin\frac{\theta_A}{2}\sin\frac{\theta_B}{2} \end{bmatrix} \tag{15}$$

In the special case of $\theta_A = \frac{\pi}{2}$ and $\theta_B = 0$, we will the original situation of the maximally entangled $|\Phi^+\rangle$ output state. The effect of applying the CNOT gate is

$$|\psi_{out}\rangle = \begin{bmatrix} 1 & 0 & 0 & 0 \\ 0 & 1 & 0 & 0 \\ 0 & 0 & 0 & 1 \\ 0 & 0 & 1 & 0 \end{bmatrix} \begin{bmatrix} \cos\frac{\theta_A}{2}\cos\frac{\theta_B}{2} \\ \cos\frac{\theta_A}{2}\sin\frac{\theta_B}{2} \\ \sin\frac{\theta_A}{2}\cos\frac{\theta_B}{2} \\ \sin\frac{\theta_A}{2}\sin\frac{\theta_B}{2} \end{bmatrix} = \begin{bmatrix} \cos\frac{\theta_A}{2}\cos\frac{\theta_B}{2} \\ \cos\frac{\theta_A}{2}\sin\frac{\theta_B}{2} \\ \sin\frac{\theta_A}{2}\sin\frac{\theta_B}{2} \\ \sin\frac{\theta_A}{2}\cos\frac{\theta_B}{2} \end{bmatrix} \tag{16}$$

The density matrix for the output state (figure 8) is:

$$\rho = \begin{bmatrix} \cos^2\frac{\theta_A}{2}\cos^2\frac{\theta_B}{2} & \frac{1}{2}\cos^2\frac{\theta_A}{2}\sin\theta_B & \frac{1}{4}\sin\theta_A\sin\theta_B & \frac{1}{2}\sin\theta_A\cos^2\frac{\theta_B}{2} \\ \frac{1}{2}\cos^2\frac{\theta_A}{2}\sin\theta_B & \cos^2\frac{\theta_A}{2}\sin^2\frac{\theta_B}{2} & \frac{1}{2}\sin\theta_A\sin^2\frac{\theta_B}{2} & \frac{1}{4}\sin\theta_A\sin\theta_B \\ \frac{1}{4}\sin\theta_A\sin\theta_B & \frac{1}{2}\sin\theta_A\sin^2\frac{\theta_B}{2} & \sin^2\frac{\theta_A}{2}\sin^2\frac{\theta_B}{2} & \frac{1}{2}\sin^2\frac{\theta_A}{2}\sin\theta_B \\ \frac{1}{2}\sin\theta_A\cos^2\frac{\theta_B}{2} & \frac{1}{4}\sin\theta_A\sin\theta_B & \frac{1}{2}\sin^2\frac{\theta_A}{2}\sin\theta_B & \sin^2\frac{\theta_A}{2}\cos^2\frac{\theta_B}{2} \end{bmatrix} \tag{17}$$

The partial trace, S(ρ^A), sums over all possible values of the second qubit. For a graphical representation of the partial trace operation, see figure 9.

$$\rho^A = \begin{bmatrix} \cos^2\frac{\theta_A}{2}\left(\cos^2\frac{\theta_B}{2} + \sin^2\frac{\theta_B}{2}\right) & 2\left(\frac{1}{4}\sin\theta_A\sin\theta_B\right) \\ 2\left(\frac{1}{4}\sin\theta_A\sin\theta_B\right) & \sin^2\frac{\theta_A}{2}\left(\cos^2\frac{\theta_B}{2} + \sin^2\frac{\theta_B}{2}\right) \end{bmatrix} = \begin{bmatrix} \cos^2\frac{\theta_A}{2} & \frac{1}{2}\sin\theta_A\sin\theta_B \\ \frac{1}{2}\sin\theta_A\sin\theta_B & \sin^2\frac{\theta_A}{2} \end{bmatrix} \tag{18}$$

Notice that in the partial trance for qubit A, the impact of B only occurs in the antidiagonal entries. In the diagonal entries, which can be thought of as a classical probability distribution that can be observed using qubit A only, the state of qubit B cannot be determined.

$$\rho^B = \begin{bmatrix} \cos^2\frac{\theta_A}{2}\cos^2\frac{\theta_B}{2} + \sin^2\frac{\theta_A}{2}\sin^2\frac{\theta_B}{2} & \frac{1}{2}\left(\cos^2\frac{\theta_A}{2} + \sin^2\frac{\theta_A}{2}\right)\sin\theta_B \\ \frac{1}{2}\left(\cos^2\frac{\theta_A}{2} + \sin^2\frac{\theta_A}{2}\right)\sin\theta_B & \cos^2\frac{\theta_A}{2}\sin^2\frac{\theta_B}{2} + \sin^2\frac{\theta_A}{2}\cos^2\frac{\theta_B}{2} \end{bmatrix} = \frac{1}{2}\begin{bmatrix} (1+\cos\theta_A\cos\theta_B) & \sin\theta_B \\ \sin\theta_B & (1-\cos\theta_A\cos\theta_B) \end{bmatrix} \quad (19)$$

The van Neumann or Entanglement entropy can be found using the eigenvalues of either partial trace

$$\lambda_\pm = \frac{1}{4}\left(2 \pm \sqrt{3 + \cos 2\theta_A - 2\cos 2\theta_B \sin^2\theta_A}\right) \quad (20)$$

and then applying eq. 9:

$$S = \frac{1}{4}\left(\mathrm{Log}[256] - 2\left(\mathrm{Log}\left[2 - \sqrt{3+\mathrm{Cos}[2a] - 2\,\mathrm{Cos}[2b]\,\mathrm{Sin}[a]^2}\right] + \mathrm{Log}\left[2 + \sqrt{3+\mathrm{Cos}[2a] - 2\,\mathrm{Cos}[2b]\,\mathrm{Sin}[a]^2}\right]\right) - 2\,\mathrm{ArcCoth}\left[\frac{2}{\sqrt{3+\mathrm{Cos}[2a] - 2\,\mathrm{Cos}[2b]\,\mathrm{Sin}[a]^2}}\right]\sqrt{3+\mathrm{Cos}[2a] - 2\,\mathrm{Cos}[2b]\,\mathrm{Sin}[a]^2}\right) \quad (21)$$

The entanglement entropy is plotted graphically in figure 10, and the "map" of the resulting states is shown in figure 11. As seen in table 3, when the control bit is changed, seemingly in conflict with our expectations of the direction of causality, it is called Phase Kickback.[48] The entropy of a joint entangled state can be less than the combined entropies of the individual wavefunctions because of the quantum correlations between them. Bell states are maximally entangled and represent 1 bit of entropy produced when measured. For example, the state $|\Phi^+\rangle = \frac{1}{\sqrt{2}}[|00\rangle + |11\rangle]$ had zero entropy as a pure state. But measuring one particle in isolation will give 0 or 1 with equal probability. It is only after comparing the results of measuring both particles that you will find that they both give the same result when measured in the standard basis.

INPUT				OUTPUT		NOTE
States		ANGLES		States		
A	B	θ_A	θ_B	A	B	
STANDARD BASIS – NOT ENTANGED						
$\|0\rangle$	$\|0\rangle$	0	0	$\|0\rangle$	$\|0\rangle$	No change
$\|0\rangle$	$\|1\rangle$	0	π	$\|0\rangle$	$\|1\rangle$	No change
$\|1\rangle$	$\|0\rangle$	π	0	$\|1\rangle$	$\|1\rangle$	
$\|1\rangle$	$\|1\rangle$	π	π	$\|1\rangle$	$\|0\rangle$	
HADAMARD BASIS – NOT ENTANGED						
$\|+\rangle$	$\|+\rangle$	π/2	π/2	$\|+\rangle$	$\|+\rangle$	No change
$\|+\rangle$	$\|-\rangle$	π/2	3 π/2	$\|-\rangle$	$\|-\rangle$	PHASE KICKBACK!
$\|-\rangle$	$\|+\rangle$	3 π/2	π/2	$\|-\rangle$	$\|+\rangle$	No change
$\|-\rangle$	$\|-\rangle$	3 π/2	3 π/2	$\|+\rangle$	$\|-\rangle$	PHASE KICKBACK!
BELL STATES – MAXIMALLY ENTANGLED						
$\|+\rangle$	$\|0\rangle$	π/2	0	$\|00\rangle + \|11\rangle$		**Bell State: B+**
$\|+\rangle$	$\|1\rangle$	π/2	π	$\|01\rangle + \|10\rangle$		**Bell State: D+**
$\|-\rangle$	$\|0\rangle$	3 π/2	0	$\|00\rangle - \|11\rangle$		**Bell State: B-**
$\|-\rangle$	$\|1\rangle$	3 π/2	π	$-\|01\rangle + \|10\rangle$		**Bell State: D-**

TABLE 3: Result generalized Bell experiment. A is the “control” qubit and B is the “target” qubit of the CNOT gate. Entangled states cannot be written as direct product of single-qubit states. See figure 11.

However, entanglement does not guarantee that a particular Bell inequality will be violated.[49] The degree of Bell violation is shown in figure 12. Even states that are partially entangled can give values that do not exceed the Bell limit.

3D-Printed Density Matrix

The density matrix for the maximally mixed state is shown in figure 13. A partially entangled state using θ_A = xxx and θ_B = xxx (Metro29) is shown in figure 14. The height represents the magnitude, and the arrows/color represents the phase.

Probability Density of Anisotropic Harmonic Oscillator

Figure 15 is simultaneously a physical representation of data, as well as an exploration of the extent and limitations of human knowledge. This piece shows the evolution of the probability density over time for a particular case: a particle rolling in an oval bowl, also known as an anisotropic 2D harmonic oscillator. The height of each figure represents the probability density – the chance that the particle will be found that that x and y position – for a single moment in time. This particle will slosh around the bowl in a state of indeterminate bliss until someone peers in, at which point it will snap into a particular definite position.

The Hamiltonian, which represents the total energy of the particle, can be written in x-y coordinates as:

$$H(x,y) = \frac{p^2}{2m} + \frac{1}{2}m\omega_x^2 x^2 + \frac{1}{2}m\omega_y^2 y^2 \tag{22}$$

Where p is the momentum of the particle ($p^2 = p_x^2 + p_y^2$), m is its mass, and ω_x and ω_y are the natural angular frequencies in the x and y directions, respectively. The Hamiltonian is separable, so the stationary state wavefunction solutions are the direct products of the 1D Harmonic oscillator functions:

$$\psi_{n_x,n_y}(x,y) = \frac{1}{\sqrt{2^{n_x}\,n_x!}}\left(\frac{m\omega_x}{\pi\hbar}\right)^{1/4} e^{-m\omega_x x^2/2\hbar} H_{n_x}\left[\sqrt{\frac{m\omega_x}{\hbar}}x\right] \frac{1}{\sqrt{2^{n_y}\,n_y!}}\left(\frac{m\omega_y}{\pi\hbar}\right)^{1/4} e^{-m\omega_y y^2/2\hbar} H_{n_y}\left[\sqrt{\frac{m\omega_y}{\hbar}}y\right] \tag{23}$$

When n_x and n_y determine the quanta in each direction.

The associated energy of each state is:

(a)

$$
\rho = \begin{array}{c} \\ \\ \end{array}
\begin{array}{cc}
 & \begin{array}{cccc} \langle\mathbf{00}| & \langle\mathbf{01}| & \langle\mathbf{10}| & \langle\mathbf{11}| \end{array} \\
 & \left(\begin{array}{cccc}
\rho_{00,00} & \rho_{00,01} & \rho_{00,10} & \rho_{00,11} \\
\rho_{01,00} & \rho_{01,01} & \rho_{01,10} & \rho_{01,11} \\
\rho_{10,00} & \rho_{10,01} & \rho_{10,10} & \rho_{10,11} \\
\rho_{11,00} & \rho_{11,01} & \rho_{11,10} & \rho_{11,11}
\end{array}\right)
\begin{array}{c} |\mathbf{00}\rangle \\ |\mathbf{01}\rangle \\ |\mathbf{10}\rangle \\ |\mathbf{11}\rangle \end{array}
\end{array}
$$

(b)

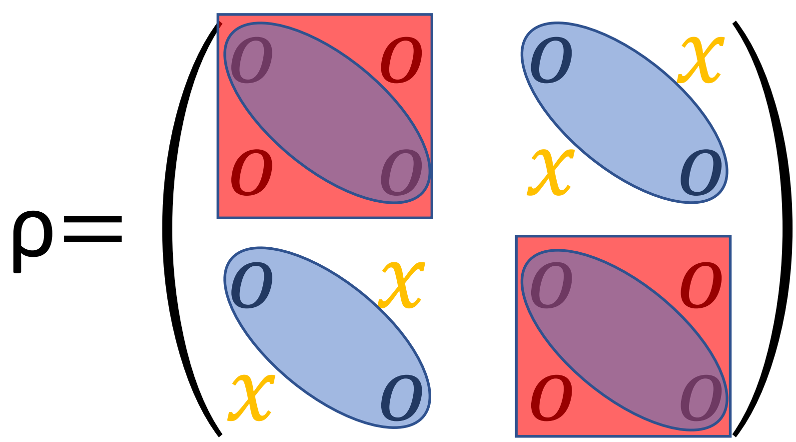

FIGURE 8: *(a) Density matrix for a pair of entangled particles expressed in the two-qubit basis {|00>, |01>,|10>,|11>} where the first value is qubit A and the second value is qubit B. (b) Representation of the computation of the partial traces ρA and ρB. Observables related with local measurements of qubit A average over the possible values of qubit B, and vice versa. The diagonal matrix elements appear in both partial traces, while the antidiagonal entries [yellow xs], which represent purely quantum mechanical bipartite correlation cross-terms, are not measurable by any one single-particle observation.*

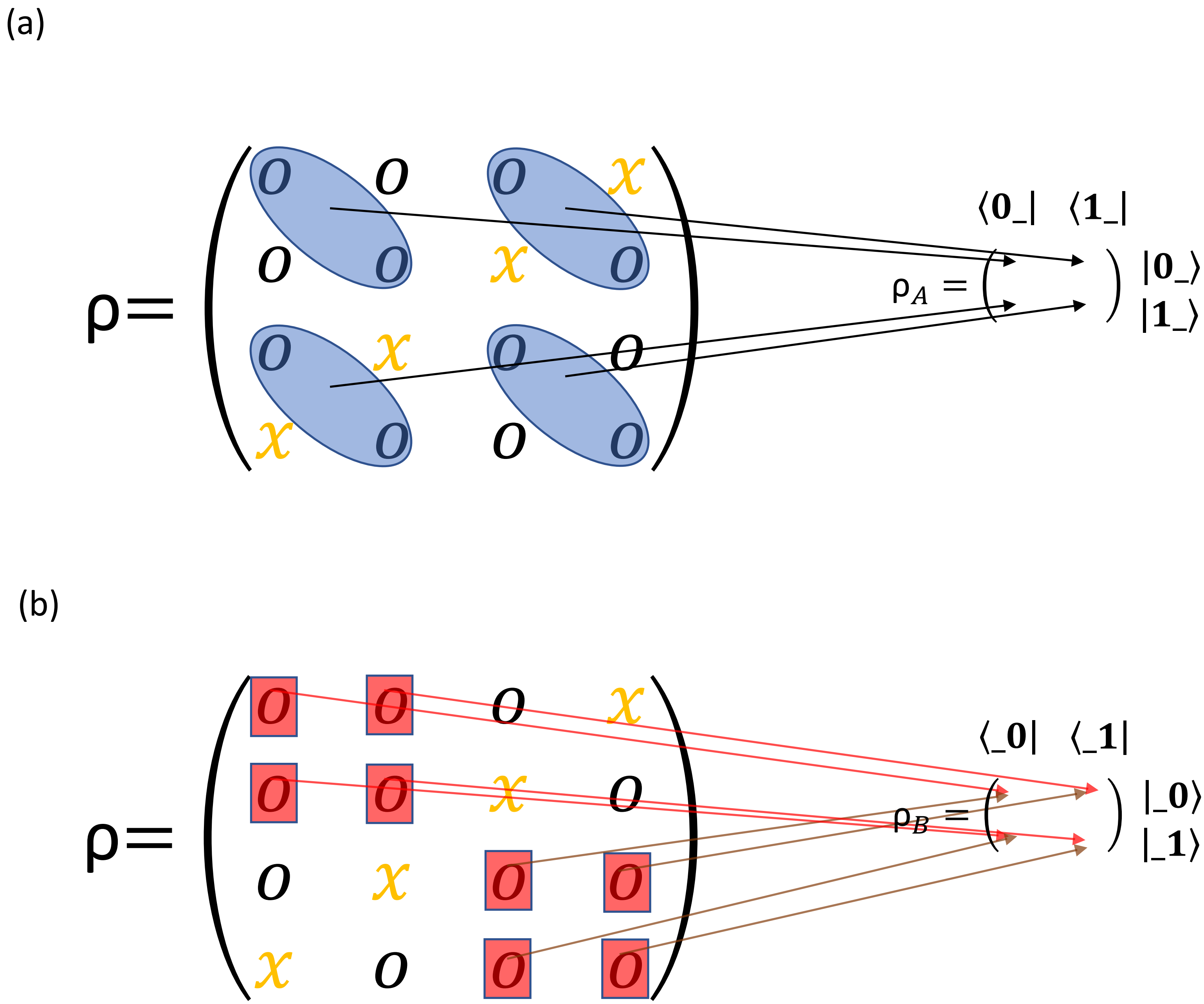

FIGURE 9: *Graphically representation of forming the partial traces. The observables of one qubit in isolation can be found by "tracing over" and summing the outcomes of the other.*

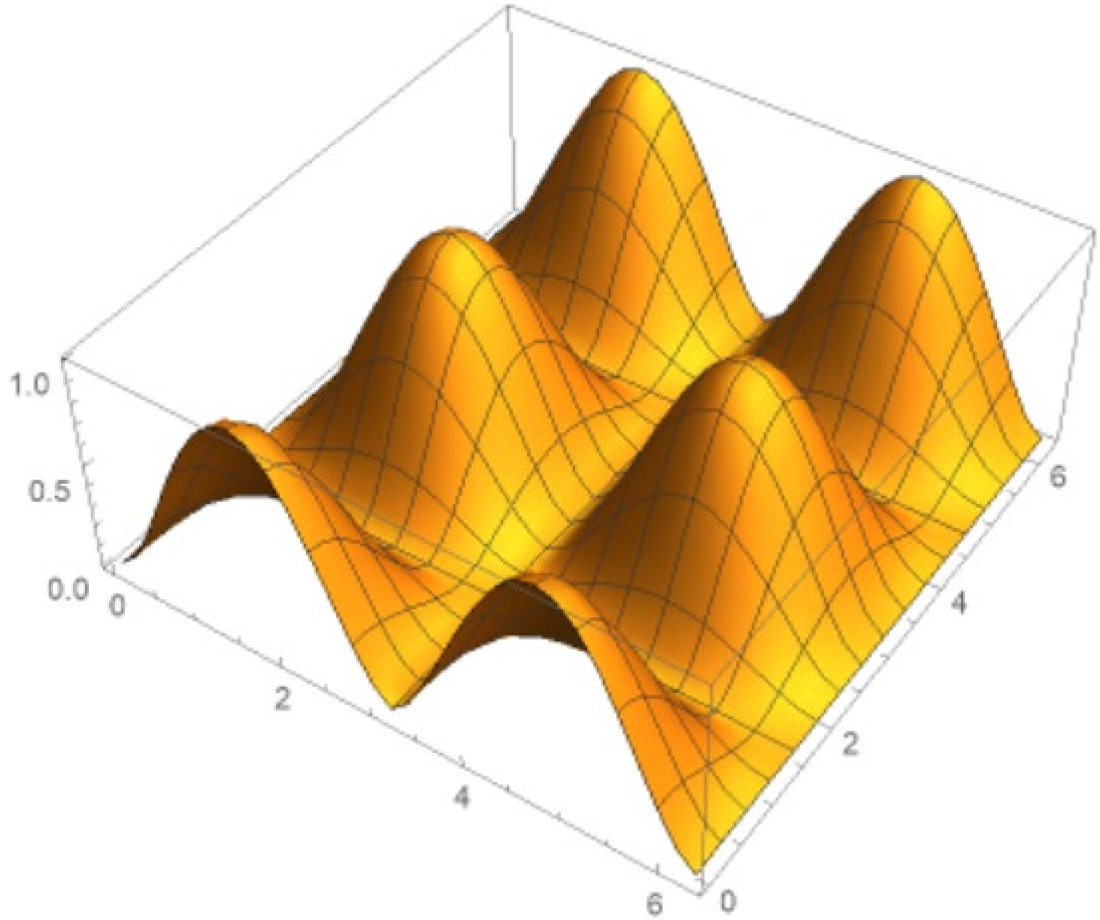

FIGURE 10: *Entanglement entropy 3D representation.*

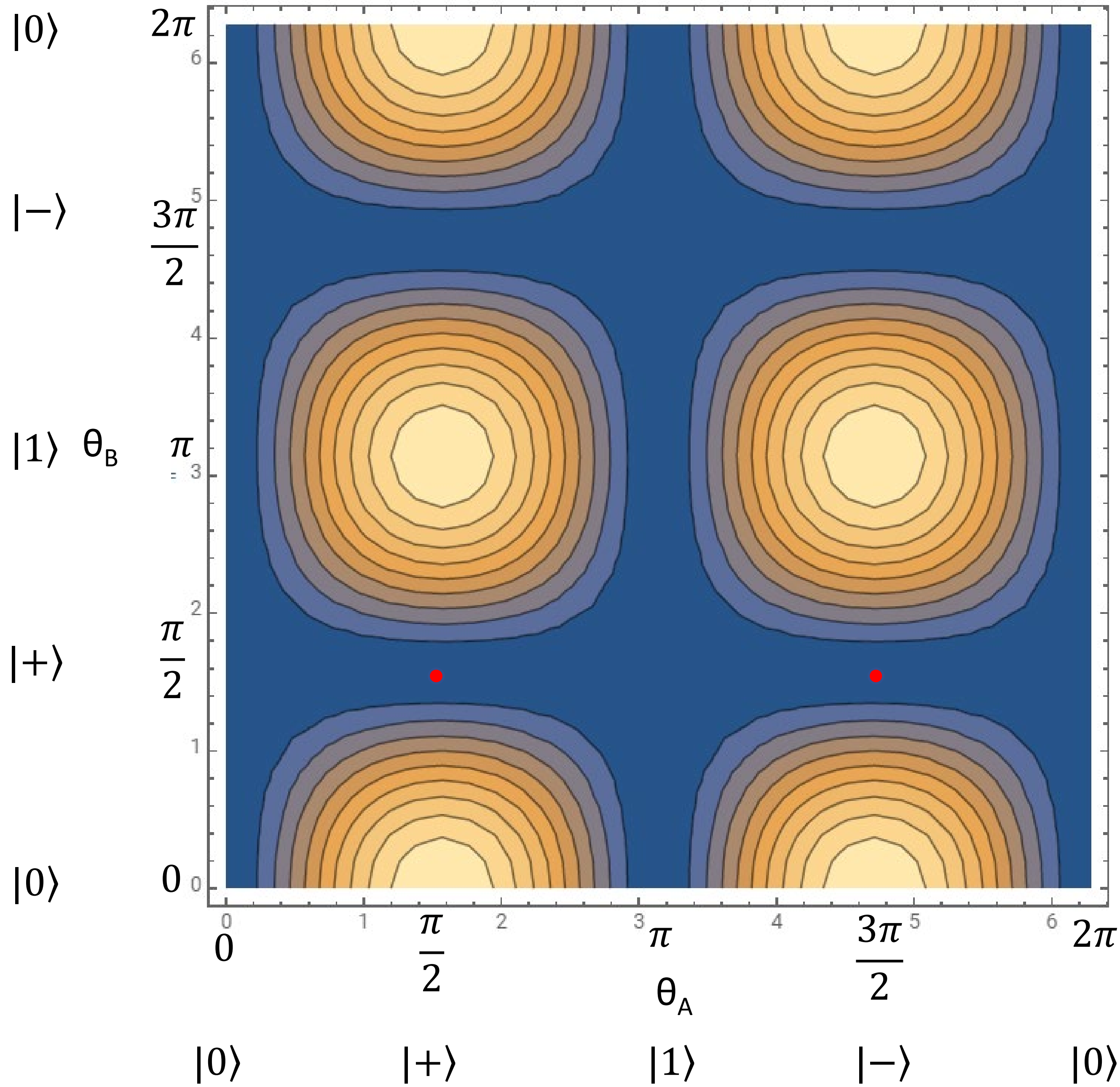

FIGURE 11: *Map of entanglement entropy. The red dots represent examples of unentangled states.*

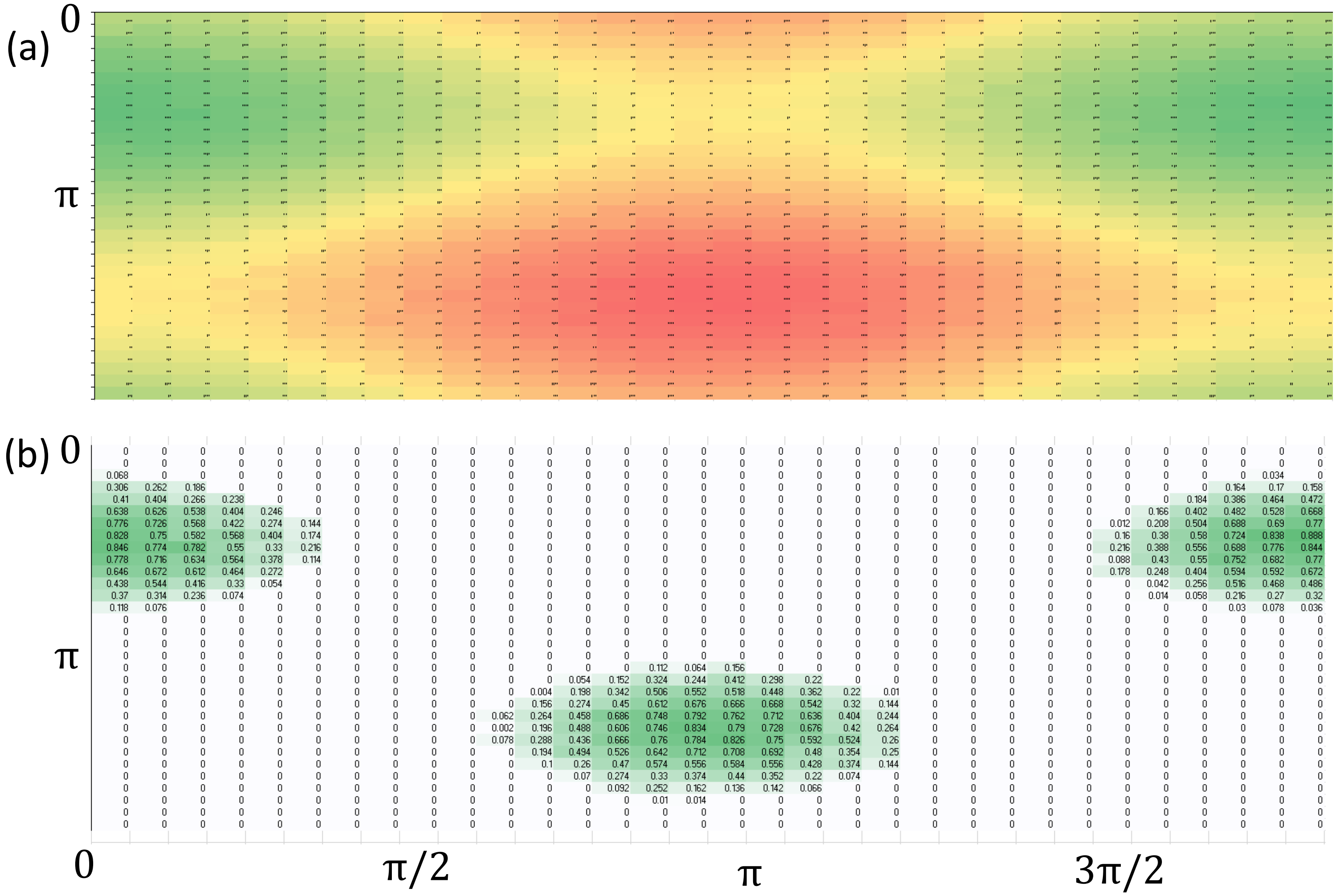

FIGURE 12: *(a) Degree of Bell violation. Some partially entangled states do not exceed the Bell limit. (b) Entangled states that violate bell's inequality.*

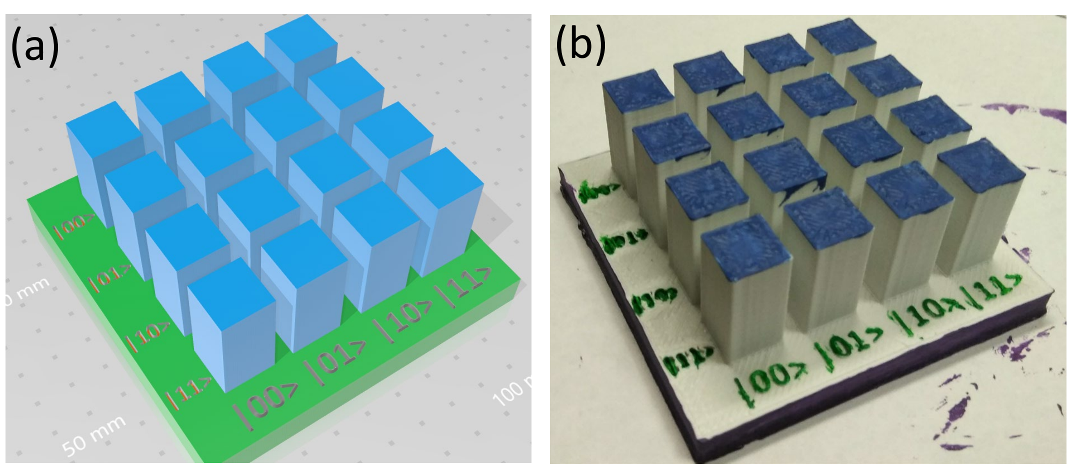

FIGURE 13: *Density matrix representation of maximally uncertain two-qubit state.*

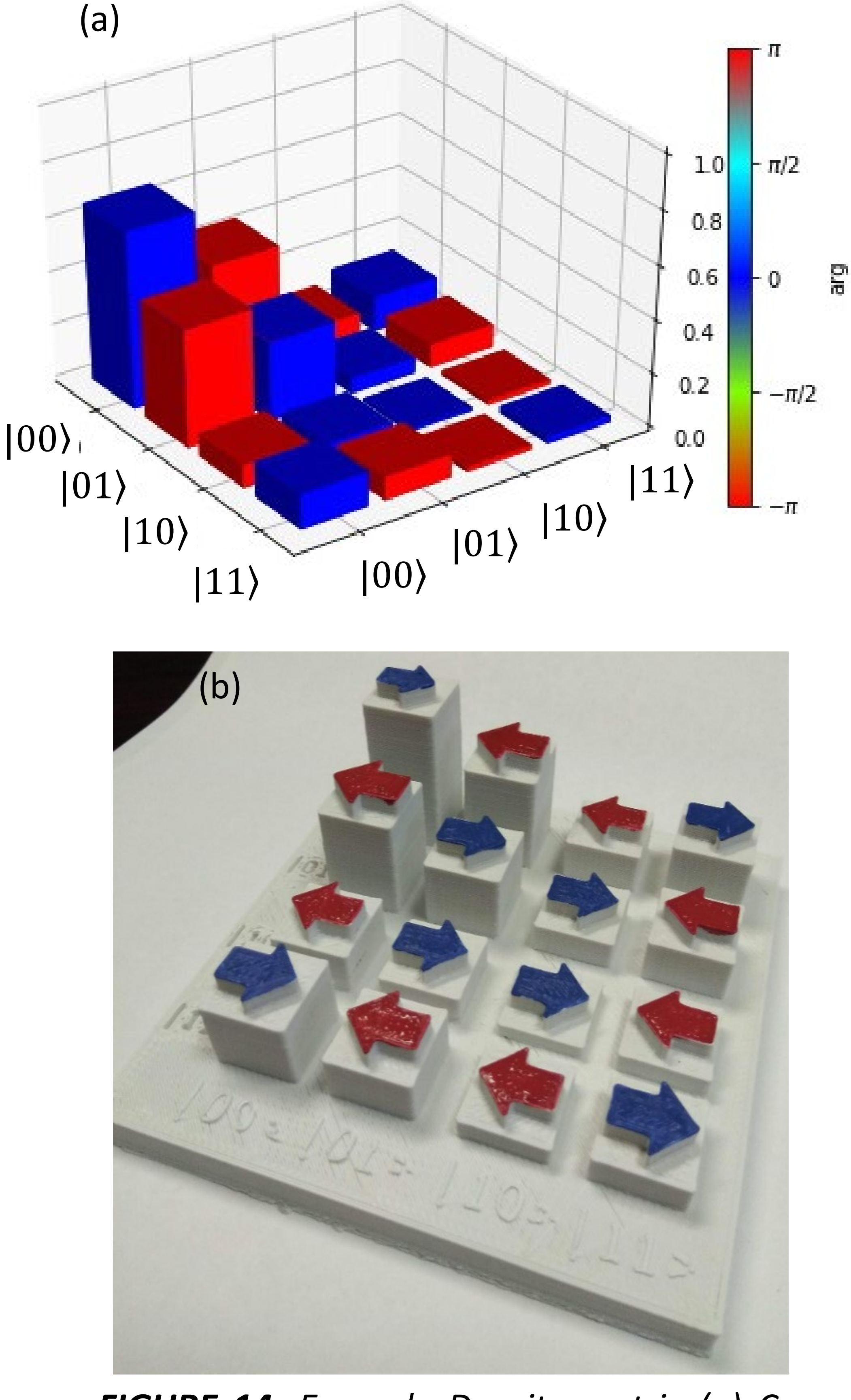

FIGURE 14: *Example Density matrix (a) Computer representation and (b) 3D-Printed model. The height shows the magnitude, which the direction of the arrow pointer and color denote the phase.*

$$E_{n_x,n_y} = \hbar\omega_x\left(n_x + \frac{1}{2}\right) + \hbar\omega_y\left(n_y + \frac{1}{2}\right) \tag{24}$$

So, the complete wavefunction is a linear combination of these states, in which the phases associated with each evolve according to $H|\psi\rangle = i\hbar\frac{\partial}{\partial t}|\psi\rangle$

$$\Phi(x,y) = \frac{\sum_{n_x,n_y} C_{n_x,n_y}\psi_{n_x,n_y}(x,y)e^{\theta_{n_x,n_y} - iE_{n_x,n_y}t/\hbar}}{\sqrt{\sum_{n_x,n_y} C^2_{n_x,n_y}}} \tag{25}$$

The probability density is the square of the wavefunction

$$\mathrm{P(x,y)} = |\Phi(x,y)|^2 \tag{26}$$

In this model, the initial conditions were:

$C_{00} = 1$ $\theta_{00} = 0$; $C_{12} = 1$ $\theta_{00} = \pi/2$; $C_{21} = 1$ $\theta_{00} = -\pi/2$

In a classical harmonic oscillator, the energy associated with each normal mode remains constant over time. In this quantum harmonic oscillator, it is similar in that the states do not mix.

Conclusion

As quantum computers transition from the laboratory to commercial applications, educating the workforce[50] needed to enable this revolution will need new pedagogical visualization tools, which can include 3D printing. The goal should be not just to convey an abstract collection of information, but rather to help guide students along the journey towards a deeply understood worldview that reflects the spirit[51] the new ways of thinking required by quantum mechanics. The work shows the value of 3D representations for this and other hard to imagine concepts.

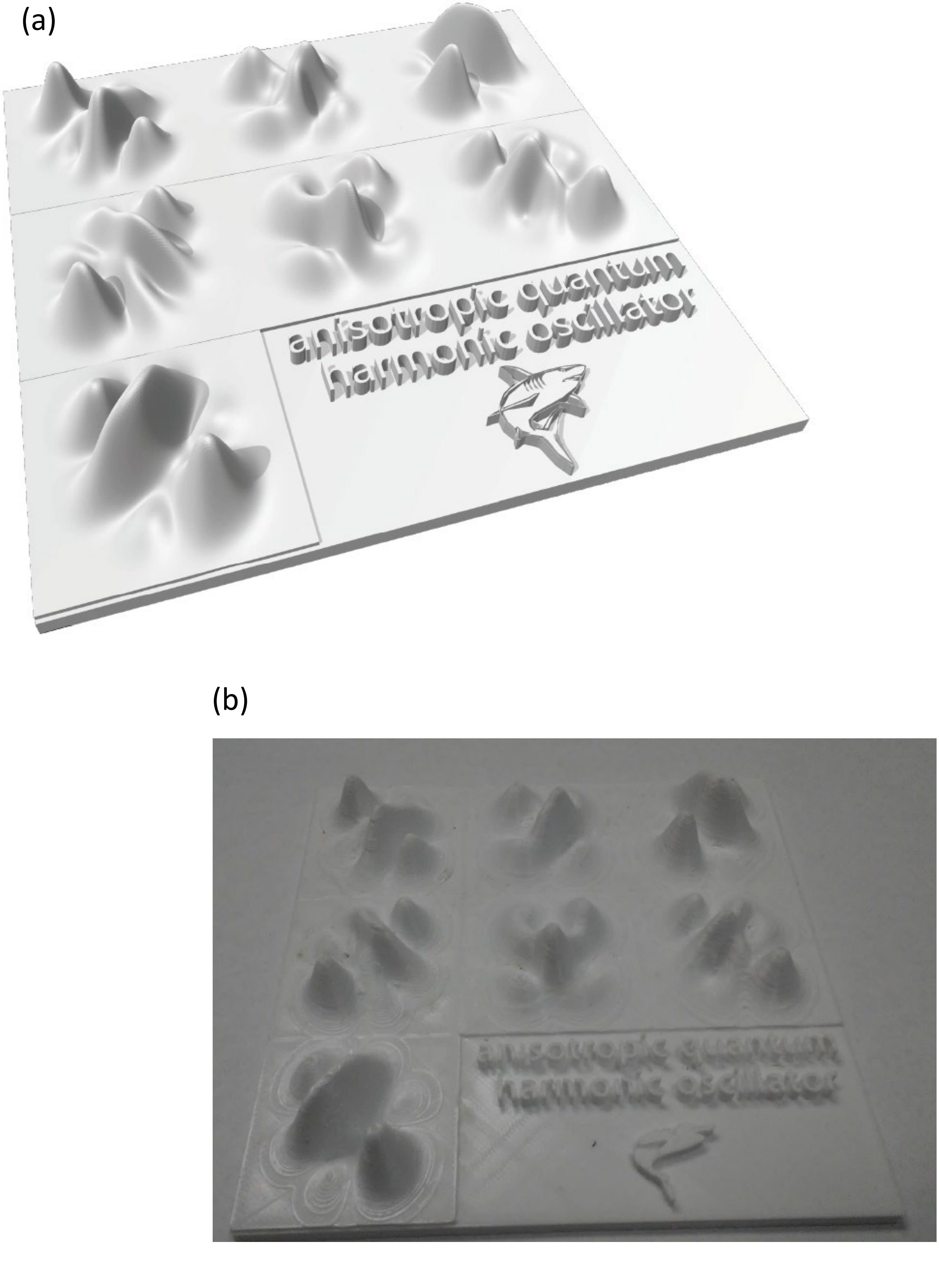

FIGURE 15: *Time evolution of single particle probability density in an anharmonic oscillator.*

- **SUPPLIMENTAL FILES**
  - **3D-Printing Files**
    - **Bell Apparatus (Fig 1)**
    - **Entanglement Entropy (Fig 11)**
    - **Density Matrix (Fig 14b)**
    - **Anisotropic Oscillator (Fig 15b)**
  - **Video Files**
    - **Bloch Sphere**
    - **Qubits**
    - **CNOT Gate**
  - **APPENDIX: Entanglement on Real Quantum Computer**

REFERENCES

[1] "Quantum Computers, Explained With Quantum Physics" 6/8/21 https://youtu.be/jHoEjvuPoB8
[2] Feynman, Richard P. "Simulating physics with computers." Int. J. Theor. Phys 21.6/7 (1982).
[3] Aaronson, S. "What Makes Quantum Computing So Hard to Explain?" 6/8/21
https://www.quantamagazine.org/why-is-quantum-computing-so-hard-to-explain-20210608/
[4] https://files.webservices.illinois.edu/9156/keyconceptsforfutureqislearners5-20.pdf
[5] Mermin, N. David. "From Cbits to Qbits: Teaching computer scientists quantum mechanics." American Journal of Physics 71.1 (2003): 23-30.
[6] Aiello, Clarice D., et al. "Achieving a quantum smart workforce." Quantum Science and Technology (2021).
[7] Economou, Sophia E., Terry Rudolph, and Edwin Barnes. "Teaching quantum information science to high-school and early undergraduate students." arXiv preprint arXiv:2005.07874 (2020).
[8] Meiksin, Judy. "Quantum materials R&D forges ahead." Mrs Bulletin 45.11 (2020): 885-888.
[9] Riedel, Max, et al. "Europe's quantum flagship initiative." Quantum Science and Technology 4.2 (2019): 020501.
[10] https://qt.eu//app/uploads/2019/02/Competence_Framework_for_QT_1.0_May2021.pdf
[11] Chhabra, Mahima, and Ritwick Das. "Quantum mechanical wavefunction: visualization at undergraduate level." European Journal of Physics 38.1 (2016): 015404.
[12] Thaller, Bernd. "Visual Tools for Quantum Mechanics Education." International Journal of Emerging Technologies in Learning (iJET) 1.2 (2006).
[13] Zaman Ahmed, Shaeema, et al. "Quantum composer: A programmable quantum visualization and simulation tool for education and research." American Journal of Physics 89.3 (2021): 307-316.
[14] Einstein, Albert, Boris Podolsky, and Nathan Rosen. "Can quantum-mechanical description of physical reality be considered complete?." Physical review 47.10 (1935): 777.
[15] Lieb, Elliott H., and Mary Beth Ruskai. "Proof of the strong subadditivity of quantum-mechanical entropy." Les rencontres physiciens-mathématiciens de Strasbourg-RCP25 19 (1973): 36-55.
[16] Bell, John S. "On the einstein podolsky rosen paradox." Physics Physique Fizika 1.3 (1964): 195.
[17] Moreau, Paul-Antoine, et al. "Imaging Bell-type nonlocal behavior." Science advances 5.7 (2019): eaaw2563.
[18] Bell, John S. "On the problem of hidden variables in quantum mechanics." Reviews of Modern Physics 38.3 (1966): 447.
[19] Convy, Ian, et al. "Mutual Information Scaling for Tensor Network Machine Learning." arXiv preprint arXiv:2103.00105 (2021).
[20] Chitambar, Eric, and Gilad Gour. "Quantum resource theories." Reviews of Modern Physics 91.2 (2019): 025001.
[21] Bello, Frank, et al. "Controlled Cavity-Free, Single-Photon Emission and Bipartite Entanglement of Near-Field-Excited Quantum Emitters." Nano Letters (2020).
[22] Wie, Chu-Ryang. "Two-qubit Bloch sphere." Physics 2.3 (2020): 383-396.
[23] Gidney, C., Marwaha, K., Haugeland, J., ebraminio, Kalra, N.: Quirk: Quantum Circuit Simulator (2021).
https://algassert.com/quirk
[24] https://quantum-computing.ibm.com/
[25] https://www.scottaaronson.com/qclec.pdf
[26] Plenio, Martin B. "The Holevo bound and Landauer's principle." Physics Letters A 263.4-6 (1999): 281-284.
[27] Rieffel, Eleanor G., and Wolfgang H. Polak. Quantum computing: A gentle introduction. MIT Press, 2011.
[28] Nemzer, Louis R. "Shannon information entropy in the canonical genetic code." Journal of theoretical biology 415 (2017): 158-170.
[29] Nemzer, Louis R. "A binary representation of the genetic code." Biosystems 155 (2017): 10-19.
[30] Jaynes, Edwin T. "Information theory and statistical mechanics." Physical review 106.4 (1957): 620.
[31] Neumaier, Arnold. "On the foundations of thermodynamics." arXiv preprint arXiv:0705.3790 (2007).
[32] Jaynes, Edwin T. "The Gibbs paradox." Maximum entropy and bayesian methods. Springer, Dordrecht, 1992. 1-21.
[33] Szilard, Leo. "On the decrease of entropy in a thermodynamic system by the intervention of intelligent beings." Behavioral Science 9.4 (1964): 301-310.

[34] Maruyama, Koji, Franco Nori, and Vlatko Vedral. "Colloquium: The physics of Maxwell's demon and information." Reviews of Modern Physics 81.1 (2009): 1.
[35] Toyabe, Shoichi, et al. "Experimental demonstration of information-to-energy conversion and validation of the generalized Jarzynski equality." Nature physics 6.12 (2010): 988-992.
[36] Shermer, Michael. "Exorcising Laplace's demon: Chaos and antichaos, history and metahistory." History and theory (1995): 59-83.
[37] Everett III, Hugh. "The theory of the universal wave function." The many-worlds interpretation of quantum mechanics. 1973.
[38] Vidick, Thomas, and Stephanie Wehner. "Does ignorance of the whole imply ignorance of the parts? Large violations of noncontextuality in quantum theory." Physical review letters 107.3 (2011): 030402.
[39] Aaronson, Scott. Quantum computing since Democritus. Cambridge University Press, 2013.
[40] Vannimenus, J., and G. Toulouse. "Theory of the frustration effect. II. Ising spins on a square lattice." Journal of Physics C: Solid State Physics 10.18 (1977): L537.
[41] Maccone, Lorenzo. "A simple proof of Bell's inequality." American Journal of Physics 81.11 (2013): 854-859.
[42] Rauch, Dominik, et al. "Cosmic Bell test using random measurement settings from high-redshift quasars." Physical Review Letters 121.8 (2018): 080403.
[43] Rosenfeld, Wenjamin, et al. "Event-ready Bell test using entangled atoms simultaneously closing detection and locality loopholes." Physical review letters 119.1 (2017): 010402.
[44] Hensen, Bas, et al. "Loophole-free Bell inequality violation using electron spins separated by 1.3 kilometres." Nature 526.7575 (2015): 682-686.
[45] Griffiths, Robert B. "Consistent histories and the interpretation of quantum mechanics." Journal of Statistical Physics 36.1 (1984): 219-272.
[46] Carroll, Sean M., and Ashmeet Singh. "Mad-dog Everettianism: Quantum mechanics at its most minimal." What is Fundamental?. Springer, Cham, 2019. 95-104.
[47] Wasak, Tomasz, Augusto Smerzi, and Jan Chwedeńczuk. "Role of Particle Entanglement in the Violation of Bell Inequalities." Scientific reports 8.1 (2018): 1-6.
[48] Johansson, Niklas, and Jan-åke Larsson. "Arrangement, system, method and computer program for simulating a quantum toffoli gate." U.S. Patent Application No. 16/607,050.
[49] W. J. Munro and K. Nemoto and A. G. White. The Bell inequality: a measure of entanglement? Journal of Modern Optics. 48 (7) 1239-1246, 2001 Doi:10.1080/095003400110034532
[50] Fox, Michael FJ, Benjamin M. Zwickl, and H. J. Lewandowski. "Preparing for the quantum revolution: What is the role of higher education?" Physical Review Physics Education Research 16.2 (2020): 020131.
[51] Raymond, Eric S., and Guy L. Steele, eds. The new hacker's dictionary. Mit Press, 1996.

Appendix: Real Quantum Computer

```python
#BELL
# quantum circuit to make a Bell state
bell = QuantumCircuit(2, 2)
bell.h(0)
bell.cx(0, 1)

meas = QuantumCircuit(2, 2)
meas.measure([0,1], [0,1])
circ = bell + meas

circ.draw(output='mpl')
```

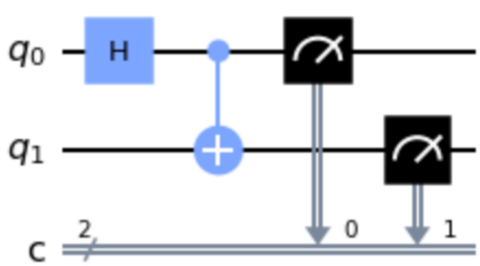

Python Code for quantum circuit using Qiskit software development kit

IBMQ Jobs

Clear

Job ID	Backend	Status	Queue	Message
60738d094ee21e70a7b01dcf	ibmq_quito	DONE	-	job has successfully run
60738ccfdf2031232705f695	ibmq_quito	DONE	-	job has successfully run
60738c06bb1d8874d708dad2	ibmq_quito	DONE	-	job has successfully run
60738ba815e37f6192151575	ibmq_quito	DONE	-	job has successfully run

IBM quantum computer job list

```
[ ] #IBM Quantum Computer
    result = execute(circ, device, shots=8000).result()
```

```
[ ] counts  = result.get_counts(circ)
    print(counts)
```

```
{'00': 3860, '01': 230, '10': 530, '11': 3380}
```

```
fixed_count= {}
all_keys=['00','01','10','11']
for key in all_keys:
  if key in counts.keys():
    fixed_count[key]=counts[key]
  else:
    fixed_count[key]=0
```

Results of 8000 trials

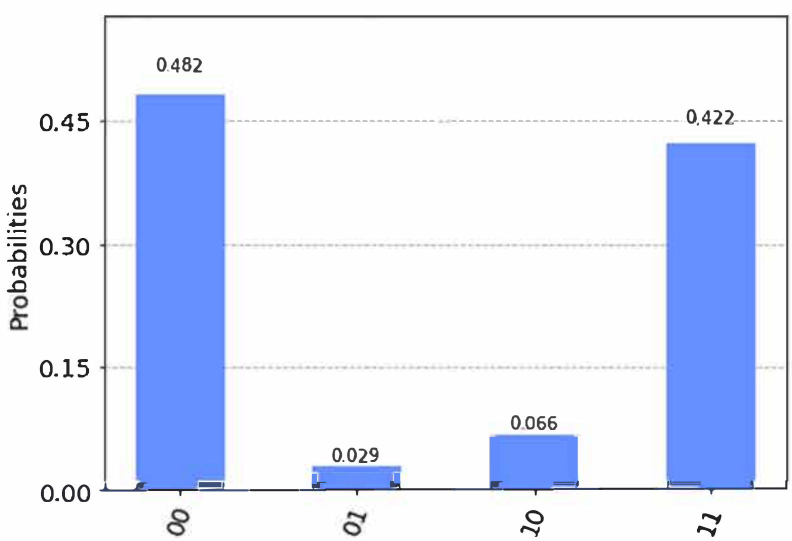

Graphical representation of results

Jobs /

60738d094ee21e70a7b01dcf

Edit Tags

Details

20.5s
Total completion time

ibmq_quito
System

Sent from	API
Created on	Apr 11, 2021 7:58 PM
Sent to queue	Apr 11, 2021 7:58 PM
Provider	ibm-q/open/main
Run mode	fairshare
# of shots	8000
# of circuits	1

Status Timeline

- Created: Apr 11, 2021 7:58 PM
- Transpiling
- Validating: 677ms
- In queue: 10s
- Running: 9.2s
  approx. time in system 8.7s
- Completed: Apr 11, 2021 7:58 PM

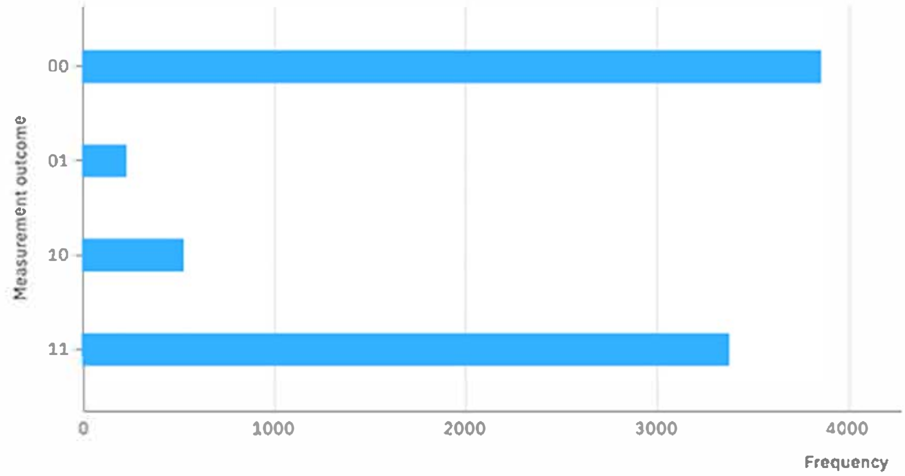

Circuit

Diagram   Qasm   Qiskit

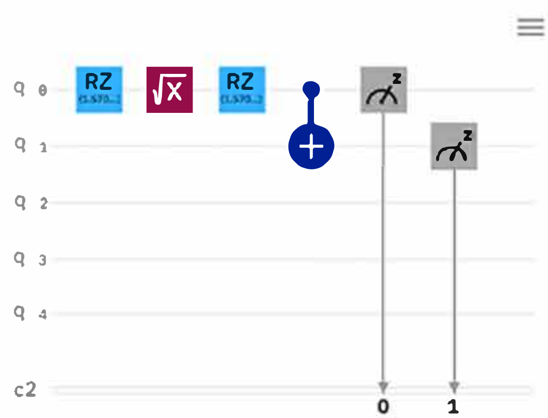

Results shown using IBM Quantum Lab online interface